

# Thermally Driven Two-Sphere Microswimmer with Internal Feedback Control

Jun Li,<sup>1,2</sup> Ziluo Zhang,<sup>2,3</sup> Zhanglin Hou,<sup>2,4</sup> Yuto Hosaka,<sup>5</sup> Kento Yasuda,<sup>6</sup> Linli He,<sup>1,\*</sup> and Shige-yuki Komura<sup>2,4,†</sup>

<sup>1</sup>*Department of Physics, Wenzhou University, Wenzhou, Zhejiang 325035, China*

<sup>2</sup>*Wenzhou Institute, University of Chinese Academy of Sciences, Wenzhou, Zhejiang 325001, China*

<sup>3</sup>*Institute of Theoretical Physics, Chinese Academy of Sciences, Beijing 100190, China*

<sup>4</sup>*Oujiang Laboratory, Wenzhou, Zhejiang 325000, China*

<sup>5</sup>*Max Planck Institute for Dynamics and Self-Organization (MPI DS), Am Faßberg 17, 37077 Göttingen, Germany*

<sup>6</sup>*Research Institute for Mathematical Sciences, Kyoto University, Kyoto 606-8502, Japan*

We investigate the locomotion of a thermally driven elastic two-sphere microswimmer with internal feedback control that is realized by the position-dependent friction coefficients. In our model, the two spheres are in equilibrium with independent heat baths characterized by different temperatures, causing a heat flow between the two spheres. We generally show that the average velocity of the microswimmer is non-zero when the friction coefficients are dependent on the spring extension. Using the method of stochastic thermodynamics, we obtain the entropy production rate and estimate the efficiency of the two-sphere microswimmer. The proposed self-propulsion model highlights the importance of information in active matter and offers a fundamental transport mechanism in various biological systems.

## I. INTRODUCTION

Microswimmers, such as sperm cells or motile bacteria, are tiny objects moving in viscous environments, and are expected to be relevant to microfluidics and microsystems [1]. By transforming chemical energy into mechanical work, microswimmers change their shapes and move in viscous fluids [2]. According to Purcell's scallop theorem, microswimmers in a Newtonian fluid need to undergo non-reciprocal body motion for steady locomotion [3, 4]. To realize such a non-reciprocal deformation, various microswimmer models that have more than two degrees of freedom have been proposed [5]. One example is the three-sphere microswimmer in which three in-line spheres are linked by two arms of varying lengths [6, 7].

Among various generalizations of the three-sphere microswimmer model [8], Hosaka *et al.* proposed an elastic three-sphere microswimmer in which the three spheres are in equilibrium with independent heat baths having different temperatures [9]. It was shown that such a stochastic microswimmer (without any prescribed deformation) can also acquire net locomotion due to thermal fluctuations, and its average velocity is proportional to the heat flow between the spheres [9]. Later, the average entropy production rate [10, 11] and the time-correlation functions [12] of the same model were calculated by some of the current authors. In particular, the existence of an antisymmetric part of the cross-correlation function reflects the broken time-reversal symmetry of this microswimmer [12].

Prior to the above thermal three-sphere microswimmer model, Kumar *et al.* proposed a model of an active elastic dimer (AED) in which the friction coefficients of the two spheres depend on their relative coordinate [13, 14]. Their model is different from the traditional Brownian ratchet models [15, 16] because the motion asymmetry is created internally and is not induced by an external periodic potential.

They found that the average velocity of an AED is proportional to the difference between the non-equilibrium noise strengths acting on the two spheres [13, 14]. Such a self-propulsion mechanism can explain, for example, the movement of helicases on DNA [17], the walking of Myosin VI on actin filaments [18], and the collective migration of cell clusters [19].

Given the modern framework of stochastic thermodynamics [20–22] and the accumulated knowledge of the thermal three-sphere microswimmer model [9–12], the AED model offers a renewed interest, especially when the two spheres have different temperatures without any non-equilibrium noises. Moreover, the internal feedback control through the position-dependent friction coefficients in the AED model is a crucial mechanism for “informational active matter” that utilizes information (measurement and feedback) instead of energy for various non-equilibrium processes [23, 24]. Recently, we have proposed models of Ornstein-Uhlenbeck information swimmers with external and internal feedback controls [25].

In this work, we simplify the original AED model to discuss a thermally driven two-sphere microswimmer with internal feedback control that is realized by the position-dependent friction coefficients. In the current model, the two spheres are in thermal equilibrium with independent heat baths having different temperatures. We show that a combination of heat transfer between the spheres and internal feedback control leads to directional locomotion in a steady state under a noisy environment. We analytically obtain the average velocity and the entropy production rate of this stochastic micro-machine by using stochastic energetics [20]. Using these results, we further estimate the efficiency of the proposed model. We consider that our model explains one of the fundamental mechanisms for transport and locomotion in various active matter and biological systems, such as the crawling motion of a cell [26, 27].

In Sec. II, we explain the model of a thermally driven elastic two-sphere microswimmer with internal feedback control. In Sec. III, we obtain the steady-state probability distribution that is further used to calculate the average velocity and the entropy production rate in Secs. IV and V, respectively.

\* Corresponding author: linlihe@wzu.edu.cn

† Corresponding author: komura@wiucas.ac.cn

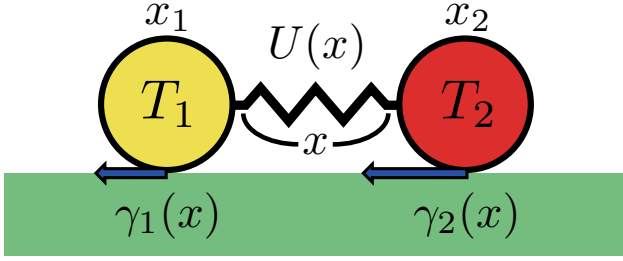


FIG. 1. (Color online) Thermally driven elastic microswimmer consisting of two hard spheres connected by a spring. The positions of the two spheres in a one-dimensional coordinate are denoted by  $x_i(t)$  ( $i = 1, 2$ ), and the spring extension is defined by  $x = x_2 - x_1$ . The spring potential energy is given by  $U(x)$ , and the two spheres are in thermal equilibrium with independent heat baths having different temperatures  $T_i$ . The friction coefficients  $\gamma_i(x)$ , acting separately on the two spheres, are dependent on the spring extension  $x$ . The internal heat flow combined with the feedback control through the position-dependent friction coefficient leads to persistent locomotion of the microswimmer.

In Sec. VI, we estimate the efficiency of the two-sphere microswimmer by using specific functional forms for the spring potential and the friction coefficients. A brief summary and discussion are given in Sec. VII.

## II. MODEL

As schematically shown in Fig. 1, we consider a microswimmer consisting of two hard spheres connected by a spring. The positions of the two spheres in a one-dimensional coordinate are denoted by  $x_i(t)$  ( $i = 1, 2$ ), and we further define the spring extension by  $x = x_2 - x_1$  that can take both positive and negative values. The spring potential energy is generally given by  $U(x)$ , which can be a harmonic potential (as we will discuss later) or that of a finitely extensible non-linear elastic (FENE) spring [14]. There are two important assumptions of the model: (i) the two spheres are in equilibrium with independent heat baths having different temperatures  $T_i$  ( $T_1 \neq T_2$ ) and (ii) the friction coefficients  $\gamma_i(x) \geq 0$ , acting separately on the two spheres, are dependent on the spring extension  $x$ . The fact that the friction coefficients  $\gamma_i(x)$  depend on the spring extension  $x$  reflects an internal feedback mechanism: as the relative position of the spheres changes, the resistance experienced by each sphere varies accordingly. This coupling allows the system to modulate its dissipative response based on internal configuration and is essential for achieving directional locomotion in the absence of external forcing. To preserve the generality of the model, we first do not specify the functional forms of  $U(x)$  and  $\gamma_i(x)$ .

The coupled overdamped Langevin equations for  $x_i$  ( $i = 1, 2$ ) under thermal noise are given by

$$\gamma_i(x)\dot{x}_i(t) = -\partial_i U(x) + g_i(x)\xi_i(t), \quad (1)$$

where  $\dot{x}_i = dx_i/dt$ ,  $\partial_i = \partial/\partial x_i$  (the summation over  $i$  is not taken here). The thermal noise  $\xi_i(t)$  has Gaussian statistics

with zero mean and unit variance:

$$\langle \xi_i(t) \rangle = 0, \quad \langle \xi_i(t)\xi_j(t') \rangle = \delta_{ij}\delta(t-t'). \quad (2)$$

According to the fluctuation-dissipation relation of the second kind, the prefactor of thermal noise is given by  $g_i(x) = \sqrt{2\gamma_i(x)k_B T_i}$ , where  $k_B$  is the Boltzmann constant [28]. The above Langevin equations are multiplicative because the noise is coupled non-linearly with the stochastic variables [29]. Then, it is necessary to specify the interpretation of the multiplicative noise (otherwise, Eq. (1) is meaningless).

Here, we employ the Itô interpretation [30], and the Langevin equation in Eq. (1) should be rewritten with the Itô convention  $x^* = x(t)$  as [14]

$$\dot{x}_i(t) = -\frac{\partial_i U(x)}{\gamma_i(x)} - \frac{[g_i(x)]^2 \partial_i \gamma_i(x)}{2[\gamma_i(x)]^3} + \frac{g_i(x^*)}{\gamma_i(x^*)} \xi_i(t). \quad (3)$$

As pointed out by Lau and Lubensky [31], the second term on the right-hand side is proportional to the temperature  $T_i$ , and it is necessary to ensure the proper thermal equilibrium. In principle, one can also choose other interpretations of the multiplicative noise, such as the Stratonovich interpretation [30], as long as the same thermal equilibrium is ensured. Using, for example, the Stratonovich convention  $x^{**} = [x(t+\Delta t) + x(t)]/2$ , where  $\Delta t$  is the small increment of time, the corresponding Langevin equation should read (see the Appendix of Ref. [14])

$$\dot{x}_i(t) = -\frac{\partial_i U(x)}{\gamma_i(x)} - \frac{g_i(x)\partial_i g_i(x)}{2[\gamma_i(x)]^2} + \frac{g_i(x^{**})}{\gamma_i(x^{**})} \xi_i(t). \quad (4)$$

Notice that Eqs. (3) and (4) statistically describe the same physical phenomena experiencing a multiplicative noise, and the second terms on the right-hand side of these equations vanish when the noise is additive, namely, when  $\gamma_i(x)$  is constant. A more general argument, including the anti-Itô convention, can be seen in the literatures [31, 32].

For the sake of mathematical convenience, we shall use the Itô interpretation and deal with the coupled Langevin equations in Eq. (3) that can be explicitly written as

$$\dot{x}_1(t) = \frac{U'(x)}{\gamma_1(x)} + \frac{k_B T_1 \gamma_1'(x)}{\gamma_1^2(x)} + \sqrt{\frac{2k_B T_1}{\gamma_1(x^*)}} \xi_1(t), \quad (5)$$

$$\dot{x}_2(t) = -\frac{U'(x)}{\gamma_2(x)} - \frac{k_B T_2 \gamma_2'(x)}{\gamma_2^2(x)} + \sqrt{\frac{2k_B T_2}{\gamma_2(x^*)}} \xi_2(t). \quad (6)$$

Hereafter, the prime denotes a derivative with respect to the relative coordinate  $x = x_2 - x_1$ , such as  $U'(x) = -\partial_1 U(x) = \partial_2 U(x)$ .

## III. STEADY-STATE PROBABILITY DISTRIBUTION

From the Langevin equations in Eqs. (5) and (6), the equations of motion for both the center-of-mass coordinate  $X = (x_1 + x_2)/2$  and the relative coordinate  $x = x_2 - x_1$  can be obtained. Since the former equation is a function of the relative coordinate  $x$  and the noise only, we first discuss the equation

of motion for  $x$  within the Itô interpretation, which is given by [14]

$$\dot{x}(t) = a(x) + b(x^*)\xi(t). \quad (7)$$

Here,  $\xi(t)$  is the superposition of  $\xi_1(t)$  and  $\xi_2(t)$  with the same Gaussian white statistics, and the two functions  $a(x)$  and  $b(x)$  are defined as

$$a(x) = -\left(\frac{1}{\gamma_1(x)} + \frac{1}{\gamma_2(x)}\right)U'(x) + k_B T_1 \left(\frac{1}{\gamma_1(x)} + \frac{\theta}{\gamma_2(x)}\right)', \quad (8)$$

$$b(x) = \sqrt{2k_B T_1 \left(\frac{1}{\gamma_1(x)} + \frac{\theta}{\gamma_2(x)}\right)}, \quad (9)$$

where we have introduced the dimensionless temperature ratio  $\theta = T_2/T_1$ . Note that  $\theta = 1$  corresponds to the thermal equilibrium.

The Fokker-Planck equation for the probability distribution  $P(x, t)$  corresponding to the Langevin equation in Eq. (7) can be written in the Itô interpretation as [33]

$$\frac{\partial}{\partial t}P(x, t) = -\frac{\partial}{\partial x}[a(x)P(x, t)] + \frac{1}{2}\frac{\partial^2}{\partial x^2}[b^2(x)P(x, t)]. \quad (10)$$

Since we are interested in the steady-state properties of the microswimmer, we discuss the steady-state probability distribution by imposing  $\partial_t P(x, t) = 0$ . Moreover, the probability flux can be set to zero since the relative coordinate is bounded by the spring potential  $U(x)$ . Then, the steady-state probability distribution  $P_s(x)$  satisfies the relation [14]

$$a(x)P_s(x) - \frac{1}{2}\frac{\partial}{\partial x}[b^2(x)P_s(x)] = 0, \quad (11)$$

and  $P_s(x)$  can be formally solved as

$$P_s(x) = \frac{\mathcal{N}}{b^2(x)} \exp\left[\int_0^x dy \frac{2a(y)}{b^2(y)}\right], \quad (12)$$

where  $\mathcal{N}$  is the normalization factor. By substituting Eqs. (8) and (9) into the above expression, we obtain [14]

$$P_s(x) = \frac{\mathcal{N}_1}{2k_B T_1} \exp\left[\int_0^x dy \left(-\frac{U'(y)[\gamma_1^{-1}(y) + \gamma_2^{-1}(y)]}{k_B T_1[\gamma_1^{-1}(y) + \theta\gamma_2^{-1}(y)]}\right)\right]. \quad (13)$$

If we further assume that the two friction coefficients are identical for all  $x$ , i.e.,  $\gamma_1(x) = \gamma_2(x)$ , the steady-state probability distribution simplifies to

$$P_s(x) = \frac{\mathcal{N}_1}{2k_B T_1} \exp\left[-\frac{2U(x)}{(1+\theta)k_B T_1}\right], \quad (14)$$

which is essentially the Boltzmann distribution modified by the temperature ratio  $\theta = T_2/T_1$ .

#### IV. AVERAGE VELOCITY

Having obtained the steady-state distribution function  $P_s(x)$  for the relative coordinate  $x$  in the previous section, we calculate the average velocity of the elastic two-sphere microswimmer. Since the center of mass velocity is simply given by  $V = \dot{X} = (\dot{x}_1 + \dot{x}_2)/2$ , we use Eqs. (5) and (6) to obtain the statistical average of  $V$  [13, 14]

$$\langle V \rangle = \frac{1}{2} \left\langle \left( \frac{1}{\gamma_1(x)} - \frac{1}{\gamma_2(x)} \right) U'(x) \right\rangle - \frac{k_B T_1}{2} \left\langle \left( \frac{1}{\gamma_1(x)} - \frac{\theta}{\gamma_2(x)} \right)' \right\rangle, \quad (15)$$

where the averaging  $\langle \dots \rangle$  is performed over the steady-state distribution  $P_s(x)$ . To derive the above expression, the contribution of the multiplicative noise terms has been omitted owing to the Itô interpretation. It should be emphasized here that  $\langle V \rangle$  vanishes when  $\theta = 1$  for any choice of  $\gamma_1(x)$  and  $\gamma_2(x)$ , provided that the average is evaluated with respect to  $P_s(x)$ .

When  $\gamma_1(x) = \gamma_2(x)$ , the above average velocity further reduces to

$$\langle V \rangle = \frac{(\theta - 1)k_B T_1}{2} \left\langle \left( \frac{1}{\gamma_1(x)} \right)' \right\rangle. \quad (16)$$

This result clearly demonstrates that the microswimmer acquires a finite average velocity when  $\theta \neq 1$  ( $T_1 \neq T_2$ ) and  $\gamma_1$  is not constant. In other words, the current microswimmer is driven by thermal energy, and the internal feedback control through  $\gamma_1(x)$  plays a crucial role for its locomotion. We remark, however, that when  $(1/\gamma_1(x))'$  and  $U(x)$  are respectively odd and even functions of  $x$ ,  $\langle V \rangle$  vanishes even if the friction coefficient is position-dependent. A similar result to Eqs. (15) and (16) was reported for an AED whose asymmetry in the non-equilibrium noise strengths leads to locomotion [13, 14]. In our study, we do not introduce any active fluctuations, which allows us to use the standard framework of stochastic thermodynamics [20–22], as we discuss below.

#### V. ENTROPY PRODUCTION RATE

In this section, we calculate the average entropy production rate of the elastic microswimmer in the steady state, which is given by

$$\langle \dot{\sigma} \rangle = -\frac{\langle \dot{Q}_1 \rangle}{T_1} - \frac{\langle \dot{Q}_2 \rangle}{T_2}, \quad (17)$$

where the stochastic heat flow  $\dot{Q}_i$  is the heat gained by the  $i$ -th sphere per unit time. According to the stochastic energetics developed by Sekimoto [20], it is given by

$$\dot{Q}_i dt = \frac{\partial U(x)}{\partial x_i} \circ dx_i, \quad (18)$$

where  $\circ$  denotes the Stratonovich product, and the small increment  $dx_i$  can be obtained from the Langevin equations in Eqs. (5) and (6). Using the Wong-Zakai theorem to deal

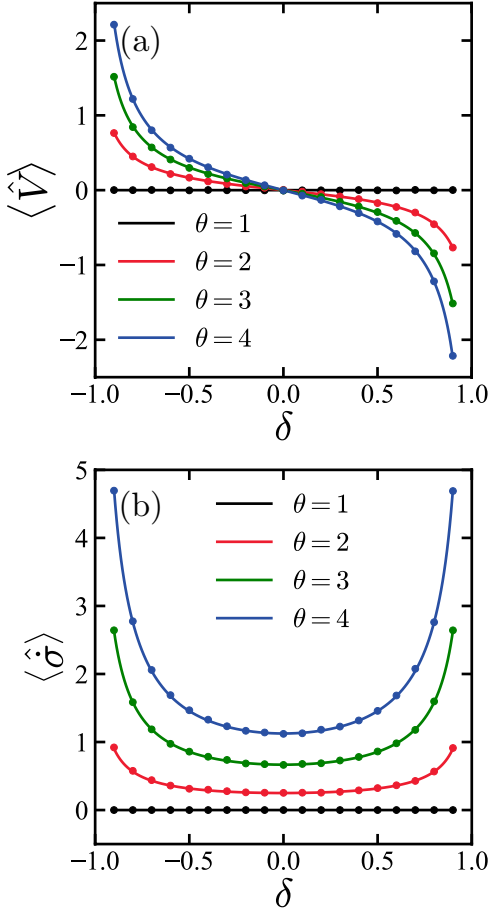


FIG. 2. (Color online) The plots of the average velocity  $\langle V \rangle$  [see Eq. (24)] and the average entropy production rate  $\langle \dot{\sigma} \rangle$  [see Eq. (25)] of the two-sphere microswimmer when the potential is  $U(x) = Kx^2/2$  and the friction coefficients are  $\gamma_1(x) = \gamma_2(x) = \gamma[1 + \delta \tanh(x/w)]$  [see Eq. (22)]. The dimensionless energy parameter is chosen here as  $\varepsilon = Kw^2/(k_B T_1) = 1$ . (a) The plot of the dimensionless average velocity  $\langle \hat{V} \rangle = \langle V \rangle \gamma / \sqrt{K k_B T_1}$  as a function of the dimensionless feedback strength parameter  $\delta$  for different values of the dimensionless temperature ratio  $\theta = T_2/T_1$ . (b) The plot of the dimensionless average entropy production rate  $\langle \hat{\sigma} \rangle = \langle \dot{\sigma} \rangle \gamma T_1 / (Kw)^2$  as a function of  $\delta$  for different values of  $\theta$ . In both (a) and (b), the filled circles correspond to the result of the numerical simulation.

with the Stratonovich product and taking the statistical average [20], we obtain after some calculation

$$\langle \hat{Q}_i \rangle = - \left\langle \frac{[U'(x)]^2}{\gamma_i(x)} \right\rangle + k_B T_i \left\langle \left( \frac{U'(x)}{\gamma_i(x)} \right)' \right\rangle. \quad (19)$$

A similar expression was obtained in Eq. (32) of Ref. [34]. When the two friction coefficients are constant and identical, the above expression reduces to Eq. (4.27) of Ref. [20].

It is straightforward to verify that  $\langle \hat{Q}_i \rangle = 0$  when  $\theta = 1$  by using the equilibrium distribution function in Eq. (13). When  $\theta \neq 1$ , we now consider the total heat flow defined by  $\langle \hat{Q} \rangle = \langle \hat{Q}_1 \rangle + \langle \hat{Q}_2 \rangle$ . Using Eqs. (8) and (9), one can generally show

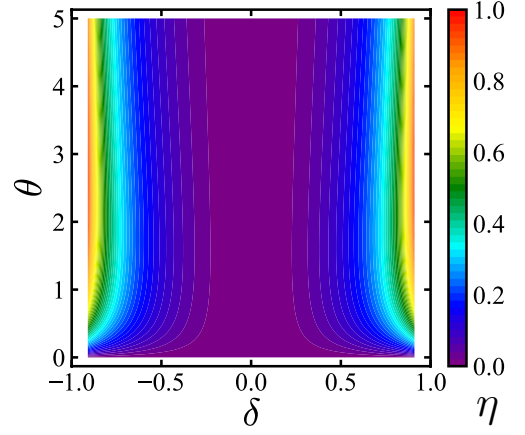


FIG. 3. (Color online) The color plot of the efficiency  $\eta$  [see Eq. (26)] of the two-sphere microswimmer as a function of the dimensionless feedback strength parameter  $\delta$  and the dimensionless temperature ratio  $\theta = T_2/T_1$ . The efficiency  $\eta$  vanishes when  $\delta = 0$ .

that  $\langle \hat{Q} \rangle$  vanishes in the steady state because

$$\langle \hat{Q} \rangle = \langle U'(x)a(x) \rangle + \frac{1}{2} \langle U''(x)b^2(x) \rangle = 0. \quad (20)$$

In the second equality, we have used Eq. (11), which stems from the steady-state condition. Notice that the relation  $\langle \hat{Q} \rangle = 0$  generally holds even if the two friction coefficients  $\gamma_1(x)$  and  $\gamma_2(x)$  are different. Since we have  $\langle \hat{Q}_2 \rangle = -\langle \hat{Q}_1 \rangle$  from Eq. (20), the average entropy production rate in Eq. (17) can be rewritten as

$$\langle \dot{\sigma} \rangle = \frac{1 - \theta \langle \hat{Q}_1 \rangle}{\theta T_1}, \quad (21)$$

which vanishes when  $\theta = 1$ . When  $T_1 < T_2$  ( $\theta > 1$ ),  $\langle \hat{Q}_1 \rangle$  is negative and we have  $\langle \dot{\sigma} \rangle > 0$ , as required from the generalized second law for non-equilibrium systems. A similar statement also holds when  $T_1 > T_2$  ( $\theta < 1$ ).

## VI. EXAMPLE

So far, we have not yet specified the functional forms of the spring potential  $U(x)$  and the friction coefficients  $\gamma_i(x)$ . As an example, we choose the harmonic potential energy  $U(x) = Kx^2/2$ , where  $K > 0$  is the spring constant, and assume that the friction coefficients have the form [13, 14]

$$\gamma_1(x) = \gamma_2(x) = \gamma[1 + \delta \tanh(x/w)], \quad (22)$$

where  $\gamma$  is a constant friction coefficient,  $\delta$  is a dimensionless feedback strength parameter satisfying  $|\delta| < 1$  (recall  $\gamma_i(x) > 0$ ), and  $w$  is a length characterizing the change of the friction coefficients. In this case, the steady-state distribution function in Eq. (14) and the average velocity in Eq. (16) become

$$P_s(x) = \sqrt{\frac{K}{\pi(1+\theta)k_B T_1}} \exp \left[ -\frac{Kx^2}{(1+\theta)k_B T_1} \right], \quad (23)$$

and

$$\langle V \rangle = \frac{\delta(1-\theta)}{2\gamma} \sqrt{\frac{Kk_B T_1}{\pi(1+\theta)}} \times \int_{-\infty}^{\infty} dz \frac{\text{sech}^2 z}{(1+\delta \tanh z)^2} \exp\left(-\frac{\varepsilon z^2}{1+\theta}\right), \quad (24)$$

respectively, where  $\varepsilon = Kw^2/(k_B T_1)$  is the dimensionless energy parameter. Note that Eq. (23) is simply a Gaussian distribution function. Since the dimensionless integral in Eq. (24) is positive (which will be evaluated numerically below),  $\langle V \rangle$  is non-zero only when  $\delta \neq 0$  and  $\theta \neq 1$ . Moreover, the temperature ratio  $\theta$  determines the direction of locomotion, i.e.,  $\langle V \rangle < 0$  when  $\delta > 0$  and  $\theta > 1$ , or vice versa. Similarly, by calculating the average heat flow  $\langle \dot{Q}_1 \rangle$  in Eq. (19), we obtain the average entropy production rate in Eq. (21) as

$$\langle \dot{\sigma} \rangle = \frac{\theta-1}{\theta} \frac{(Kw)^2}{\gamma T_1} \sqrt{\frac{\varepsilon}{\pi(1+\theta)}} \int_{-\infty}^{\infty} dz \left[ \frac{z^2}{1+\delta \tanh z} + \frac{\delta z \text{sech}^2 z}{\varepsilon(1+\delta \tanh z)^2} - \frac{1}{\varepsilon(1+\delta \tanh z)} \right] \exp\left(-\frac{\varepsilon z^2}{1+\theta}\right), \quad (25)$$

which includes another dimensionless integral.

In Fig. 2(a), we numerically plot the dimensionless average velocity  $\langle \hat{V} \rangle = \langle V \rangle \gamma / \sqrt{Kk_B T_1}$  from Eq. (24) as a function of the feedback strength parameter  $\delta$  for different values of the temperature ratio  $\theta = T_2/T_1 > 1$  when  $\varepsilon = 1$ . To confirm our analytical prediction, we have also performed numerical simulations of the coupled stochastic equations in Eqs. (5) and (6). These Langevin equations were discretized according to the Itô convention. We find a good agreement between the theoretical and numerical results. Notice that  $\langle \hat{V} \rangle$  vanishes when either  $\theta = 1$  or  $\delta = 0$ , as shown in Eq. (24). Moreover,  $\langle \hat{V} \rangle$  is an odd function of  $\delta$  because the sign of  $\delta$  determines the direction of locomotion. In Fig. 2(b), on the other hand, we numerically plot the dimensionless average entropy production rate  $\langle \hat{\sigma} \rangle = \langle \dot{\sigma} \rangle \gamma T_1 / (Kw)^2$  from Eq. (25) as a function of the feedback strength  $\delta$ . For  $\theta > 1$ ,  $\langle \hat{\sigma} \rangle$  is positive and is an even function of  $\delta$ . As a result, the entropy production rate is minimized at  $\delta = 0$  and the corresponding expression is given by  $\langle \hat{\sigma} \rangle_{\min} = k_B K (\theta - 1)^2 / (2\gamma\theta) \geq 0$ .

At this stage, it is worth evaluating the efficiency of the current microswimmer defined by [7, 11]

$$\eta = \frac{2\gamma \langle V \rangle^2}{\langle \dot{\sigma} \rangle T^*}, \quad (26)$$

where  $T^* = (T_1 + T_2)/2$  is the average temperature although either  $T_1$  or  $T_2$  can also be used. The factor  $2\gamma$  in the numerator reflects the fact that the microswimmer consists of two spheres with the same average friction coefficient  $\gamma$ . In Fig. 3, we color-plot the efficiency  $\eta$  as a function of the feedback strength parameter  $\delta$  and the temperature ratio  $\theta = T_2/T_1$ . The efficiency  $\eta$  vanishes when  $\delta = 0$  and is an even function of  $\delta$  when  $\theta$  is fixed. It is worth noting that, in the equilibrium limit of  $\theta \rightarrow 1$ , the efficiency  $\eta$  is finite because both  $\langle V \rangle$  and  $\langle \dot{\sigma} \rangle$  vanish in this limit [see Eqs. (24) and (25)].

In general, there is a contribution to the total entropy production rate coming from the center-of-mass diffusion [11], which is neglected in Eq. (26). Here, we have only considered the entropy production rate due to the heat flow [see Eq. (17)] that causes the unidirectional locomotion.

## VII. SUMMARY AND DISCUSSION

To summarize, we have studied the locomotion of a thermally driven elastic two-sphere microswimmer that has position-dependent friction coefficients. Such a microswimmer can acquire non-zero average velocity in the steady state due to the heat flow between the spheres. We have obtained the entropy production rate and further estimated the efficiency of the microswimmer. The proposed self-propulsion mechanism emphasizes the importance of active matter and biological systems driven by internal feedback control. In the future, we will calculate the time-correlation functions of the microswimmer to quantitatively discuss the degree of broken time-reversal symmetry [12].

In our model, the state-dependent friction coefficients play an essential role. The change in the friction coefficient can be caused, for example, by the change in the particle size. In this sense, the current model has a similarity to the model of “pushmepullyou” by Avron *et al.* [35] or the two-sphere model by Pandey *et al.* [36]. The main difference in our model is that the spheres have different temperatures and thermal fluctuations cause the locomotion in a stochastic manner. The internal heat flow combined with the feedback control through the position-dependent friction coefficient is the main driving force for persistent locomotion.

The other important assumption of the model is that the statistical properties of the two spheres are characterized by two different temperatures. Such a micromachine is conceptually motivated by Feynman’s Brownian ratchet [37] or a model system that interacts with two thermal environments [20]. More recently, a similar non-equilibrium dimer model confined between two walls was discussed to calculate probability flux loops that demonstrate the broken detailed balance when the temperatures are different [38–40]. In the previous thermally driven three-sphere microswimmer model [9], all the spheres were assumed to have different temperatures.

Although it is technically challenging to introduce different temperatures in a moving microswimmer, one possible way is to use a chemically heterogeneous particle, such as a Janus particle, under laser irradiation, which induces inhomogeneous temperature distribution on the particle [40]. By further introducing the internal deformation degree of freedom [41], we expect that the proposed thermally driven two-sphere microswimmer can be experimentally realized. It should be mentioned, however, that any difference in the fluctuation (both thermal and non-thermal) between the two spheres is sufficient to induce a non-zero velocity of the two-sphere microswimmer [13, 14]. Hence, rather than the thermodynamic temperature itself, an effective temperature that reflects the microswimmer’s internal fluctuation is more important for its persistent locomotion.

## ACKNOWLEDGMENTS

We thank Z. Xiong for the useful discussions. Z.H., L.H. and S.K. acknowledge the support by the National Natural Science Foundation of China (Nos. 12104453, 22273067, 12274098, and 12250710127). Y.H. acknowledges support from JSPS Overseas Research Fellowships (Grant No.

202460086). S.K. acknowledges the startup grant of Wenzhou Institute, University of Chinese Academy of Sciences (No. WIUCASQD2021041). K.Y and S.K. acknowledge the support by the Japan Society for the Promotion of Science (JSPS) Core-to-Core Program “Advanced core-to-core network for the physics of self-organizing active matter” (No. JPJSCCA20230002). J.L. and Z.Z. contributed equally to this work.

- 
- [1] E. Lauga, *The Fluid Dynamics of Cell Motility* (Cambridge University Press, 2020).
- [2] Y. Hosaka and S. Komura, Nonequilibrium transport induced by biological nanomachines, *Biophys. Rev. Lett.* 17, 51 (2022).
- [3] E. M. Purcell, Life at low Reynolds number, *Am. J. Phys.* 45, 3 (1977).
- [4] K. Ishimoto and M. Yamada, A coordinate-based proof of the scallop theorem, *SIAM J. Appl. Math.* 72, 1686 (2012).
- [5] E. Lauga and T. R. Powers, The hydrodynamics of swimming microorganisms, *Rep. Prog. Phys.* 72, 096601 (2009).
- [6] A. Najafi and R. Golestanian, Simple swimmer at low Reynolds number: Three linked spheres, *Phys. Rev. E* 69, 062901 (2004).
- [7] R. Golestanian and A. Ajdari, Analytic results for the three-sphere swimmer at low Reynolds number, *Phys. Rev. E* 77, 036308 (2008).
- [8] K. Yasuda, Y. Hosaka, and S. Komura, Generalized three-sphere microswimmers, *J. Phys. Soc. Jpn.* 92, 121008 (2023).
- [9] Y. Hosaka, K. Yasuda, I. Sou, R. Okamoto, and S. Komura, Thermally driven elastic micromachines, *J. Phys. Soc. Jpn.* 86, 113801 (2017).
- [10] I. Sou, Y. Hosaka, K. Yasuda, and S. Komura, Nonequilibrium probability flux of a thermally driven micromachine, *Phys. Rev. E* 100, 022607 (2019).
- [11] I. Sou, Y. Hosaka, K. Yasuda, and S. Komura, Irreversibility and entropy production of a thermally driven micromachine, *Physica A* 562, 125277 (2021).
- [12] J. Li, Z. Zhang, Z. Hou, K. Yasuda, and S. Komura, Time-correlation functions of stochastic three-sphere micromachines, *Phys. Rev. E* 110, 044603 (2024).
- [13] K. V. Kumar, S. Ramaswamy, and M. Rao, Active elastic dimers: Self-propulsion and current reversal on a featureless track, *Phys. Rev. E* 77, 020102(R) (2008).
- [14] A. Baule, K. V. Kumar, and S. Ramaswamy, Exact solution of a Brownian inchworm model for self-propulsion, *J. Stat. Mech.*, P11008 (2008).
- [15] F. Jülicher, A. Ajdari, and J. Prost, Modeling molecular motors, *Rev. Mod. Phys.* 69, 1269 (1997).
- [16] P. Reimann, Brownian motors: noisy transport far from equilibrium, *Phys. Rep.* 361, 57 (2002).
- [17] J. Yu, T. Ha, and K. Schulten, How directional translocation is regulated in a DNA helicase motor, *Biophys. J.* 91, 2097 (2006).
- [18] D. Altman, H. L. Sweeney, and J. A. Spudis, The mechanism of Myosin VI translocation and its load-induced anchoring, *Cell* 116, 737 (2004).
- [19] D.-L. Pagès, E. Dornier, J. de Seze, E. Gontran, A. Maitra, A. Maciejewski, L. Wang, R. Luan, J. Cartry, C. Canet-Jourdan, J. Raingeaud, G. Lemahieu, M. Lebel, M. Ducreux, M. Gelli, J.-Y. Scazec, M. Coppey, R. Voituriez, M. Piel, F. Jaulin, Cell clusters adopt a collective amoeboid mode of migration in confined nonadhesive environments, *Sci. Adv.* 8, eabp8416 (2022).
- [20] K. Sekimoto, *Stochastic Energetics* (Springer, Berlin Heidelberg, 2010).
- [21] C. Jarzynski, Equalities and Inequalities: Irreversibility and the Second Law of Thermodynamics at the Nanoscale, *Annu. Rev. Condens. Matter Phys.* 2, 329 (2011).
- [22] U. Seifert, Stochastic thermodynamics, fluctuation theorems and molecular machines, *Rep. Prog. Phys.* 75, 126001 (2012).
- [23] B. VanSaders and V. Vitelli, Informational active matter, arXiv:2302.07402.
- [24] C. Huang, M. Ding, and X. Xing, Information swimmer: Self-propulsion without energy dissipation, *Phys. Rev. Res.* 2, 043222 (2020).
- [25] Z. Hou, Z. Zhang, J. Li, K. Yasuda, and S. Komura, Ornstein-Uhlenbeck information swimmers with external and internal feedback controls, *EPL* 150, 27001 (2025).
- [26] M. Leoni and P. Sens, Model of cell crawling controlled by mechanosensitive adhesion, *Phys. Rev. Lett.* 118, 228101 (2017).
- [27] M. Tarama and R. Yamamoto, Mechanics of cell crawling by means of force-free cyclic motion, *J. Phys. Soc. Jpn.* 87, 044803 (2018).
- [28] M. Doi, *Soft Matter Physics* (Oxford University, Oxford, 2013).
- [29] N. G. van Kampen, *Stochastic Processes in Physics and Chemistry* (North-Holland, Amsterdam, 2007).
- [30] V. Gardiner, *Stochastic Methods* (Springer, Berlin, 2009).
- [31] A. W. C. Lau and T. C. Lubensky, State-dependent diffusion: Thermodynamic consistency and its path integral formulation, *Phys. Rev. E* 76, 011123 (2007).
- [32] T. Kuroiwa and K. Miyazaki, Brownian motion with multiplicative noises revisited, *J. Phys. A: Math. Theor.* 47, 012001 (2014).
- [33] H. Risken, *The Fokker-Planck Equation: Methods of Solution and Applications* (Springer, Berlin, 1996).
- [34] M. E. Cates, É. Fodor, T. Markovich, C. Nardini, and E. Tjhung, Stochastic hydrodynamics of complex fluids: Discretisation and entropy production, *Entropy* 24, 254 (2022).
- [35] J. E. Avron, O. Kenneth, and D. H. Oaknin, Pushmepullyou: an efficient micro-swimmer, *New J. Phys.* 7, 234 (2005).
- [36] A. Pandey and R. A. Simha, Minimal polar swimmer at low Reynolds number, *Eur. Phys. J. E* 35, 52 (2012).
- [37] R. P. Feynman, R. B. Leighton, M. Sands, *The Feynman Lectures on Physics, Vol. I* (Addison-Wesley, Reading, MA, 1966).
- [38] C. Battle, C. P. Broedersz, N. Fakhri, V. F. Geyer, J. Howard, C. F. Schmidt, and F. C. MacKintosh, Broken detailed balance at mesoscopic scales in active biological systems, *Science* 352, 604 (2016).
- [39] F. S. Gnesotto, F. Mura, J. Gladrow, and C. P. Broedersz, Broken detailed balance and non-equilibrium dynamics in living systems: a review, *Rep. Prog. Phys.* 81, 066601 (2018).
- [40] J. Li, J. M. Horowitz, T. R. Gingrich, and N. Fakhri, Quantifying dissipation using fluctuating currents, *Nat. Commun.* 10, 1666 (2019).

- [41] M. Yang, A. Wysocki, and M. Ripoll, Hydrodynamic simulations of self-phoretic microswimmers, *Soft Matter* 10, 6208 (2014).